SNOWMELT RUNOFF SIMULATION USING A DEGREE-DAY AND NONLINEAR MULTIPLE RECESSION MODEL

BY

Sung KIM*, John R. BUSCH**, and Myron MOLNAU**

INTRODUCTION

In conceptual watershed modeling, the water input is usually separated into a number of components (e.g. surface runoff, subsurface runoff, groundwater runoff, etc.) through a number of zones (e.g. impervious area, upper zone, lower zone, etc.). Each component is routed separately using a routing method (e.g. unit hydrograph, linear reservoir(s), etc.), and each component is then added to compute the total runoff. This elaborate "separating-and-adding" structure has some weaknesses as pointed out by Klemeš (1983).

> The greatest weakness of the present generation of these models (common conceptual watershed models) is their structural arbitrariness and over specification. . . . Given enough parameters related to volumetric and time changes, this procedure seldom fails (as far as the past hydrologic record is concerned) because, in essence, it is not different from making a high-degree polynomial fit a segment of given curve.

In snowmelt runoff modeling, less elaborate structures have been also reported to describe the water transport process. Using a runoff recession coefficient, Gartska et al. (1958) showed that the snowmelt runoff hydrograph is a superimposition of the "daily-hydrograph". Martinec (1963, 1965) reported a simple snowmelt runoff model using the concepts of superimposition and a recession coefficient. Later, a nonlinear recession coefficient and snow-coverage information were incorporated by Martinec (1975), and Martinec et al. (1983) reported as the Snowmelt-Runoff Model (SRM). The SRM has been applied successfully to basins ranging in size from 2.65 km^2 to 4,000 km^2 (Martinec et al., 1983), and according to Rango and Martinec (1981), the accuracy of simulation generally decreases as the basin size increases. In the SRM, the water input is routed using a single recession process and a nonlinear recession coefficient.

In this paper, a simple snowmelt model is derived by using the concepts of superimposition and three nonlinear recession coefficients. In addition, snow coverage observations are utilized indirectly to adjust the degree-day factor. The process is applied to a large semi-arid basin, the Snake River basin above Heise, Idaho (14,900 km^2) for 11 snowmelt seasons (1972-1982).

RUNOFF ROUTING

The runoff hydrograph has been characterized by recessions (Barnes, 1939; Toebes and Strang, 1964; Dunne and Black, 1971), and, generally, three different components have been recognized: surface runoff, interflow and baseflow recessions (Fig.1). If an effective water input, I_n, during a unit period, Δt, produces an instantaneous hydrograph as shown in Fig.2, and the hydrograph usually have a quick recession coefficient, $k1_n$, in the first u number of the unit period, $u\Delta t$, a moderate recession coefficient, $k2_n$, in the following v number of the unit period, $v\Delta t$, and a slow recession coefficient, $k3_n$, in the remaining period.

It should be noted that these three recession responses do not necessarily represent the conventional runoff responses, such as surface runoff recession, interflow recession, and baseflow recession. Instead, these responses only represent sequential recession reponses in the outflow hydrograph regardless of paths of runoff. Each recession coefficient in period n is a decreasing ratio of a runoff element (e.g. a "daily-contributed-runoff" and not the total runoff) occurring in period n to that occurring in period n+1. The intermediate recession coefficients, $k12_n$ and $k23_n$,

Presented at the 54th Western Snow Conference, April 15-17, 1986, Phoenix, Arizona.
* Research Associate, ** Professors, Agricultural Engineering Department, University of Idaho, Moscow, ID 83843.

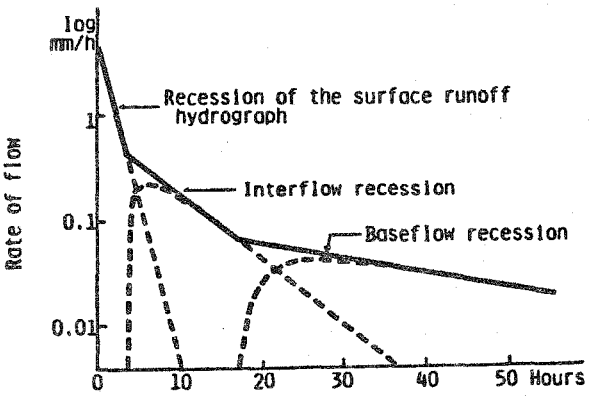

Fig. 1. Illustration of reccsion curves (after Raudkivi, 1974).

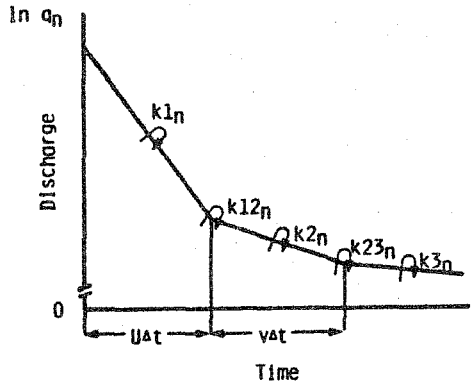

Fig. 2. Illustration of the three recession curves with three recession periods.

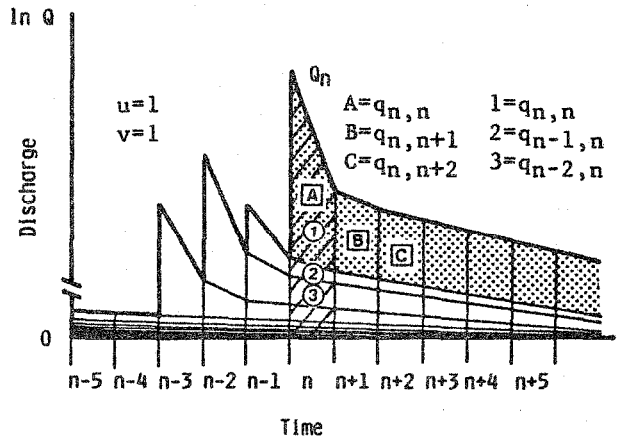

Fig. 3. Illustration for the summation of runoff elements.

represent the relationships between the adjacent recession periods. Each defined recession coefficient is a variable which is determined by the runoff rate or by other recession coefficients.

The mass balance of the input and output (the sum of runoff originated from the effective water input, I_n, equal to I_n) can be expressed as:

$$I_n = \sum_{j=0}^{u-1} q_{n,n+j} + \sum_{j=u}^{u+v-1} q_{n,n+j} + \sum_{j=u+v}^{\infty} q_{n,n+j} \qquad (1)$$

where u and v indicate the first and second recession periods, respectively (Fig.2), and $q_{n1,n2}$ denotes the runoff element originated from the input in period n1, I_{n1}, and contributes to the total runoff in period n2, Q_{n2} (Fig.3). Kim (1986) has solved Eq.1 using the three recession coefficients.

$$\frac{I_n}{q_{n,n}} = \frac{1 - k1_n^u}{1 - k1_n} + \frac{k1_n^{u-1} k12_n (1 - k2_n^v)}{1 - k2_n} + \frac{k1_n^{u-1} k12_n k2_n^{v-1} k23_n}{1 - k3_n} \qquad (2)$$

If

$$\lambda_n = q_{n,n} / I_n \qquad (3)$$

the variable λ_n denotes the ratio of the runoff element $q_{n,n}$ to the input I_n.

Therefore, the total runoff in period n, Q_n, can be expressed as the sum of runoff elements contributing to the runoff in period n, ($q_{n,n}$, $q_{n-1,n}$, $q_{n-2,n}$, . . ., $q_{n-\infty,n}$), as illustrated in Fig.3:

$$Q_n = \sum_{j=0}^{u-1} q_{n-j,n} + \sum_{j=u}^{u+v-1} q_{n-j,n} + \sum_{j=u+v}^{\infty} q_{n-j,n} \qquad (4)$$

Eq.4 can be rewritten using the recession coefficients and the variable λ_i (Kim, 1986).

$$Q_n = \sum_{j=0}^{u-1} k1_{n-j}^{j} \lambda_{n-j} I_{n-j} + \sum_{j=u}^{u+v-1} k1_{n-j}^{u-1} k12_{n-j} k2_{n-j}^{j-u} \lambda_{n-j} I_{n-j} + \sum_{j=u+v}^{\infty} k1_{n-j}^{u-1} k12_{n-j} k2_{n-j}^{v-1} k23_{n-j} k3_{n-j}^{j-u-v} \lambda_{n-j} I_{n-j} \qquad (5)$$

The three separate terms in Eq.5 represent the sum of runoff elements from the first, second, and third recession periods using the recession coefficients and inputs. A number of different types of equations (e.g. linear, nonlinear, single recession, two recession, etc.) can be derived by limiting either the recession periods or the recession coefficients as shown in Fig.4. A recursive form of the first example in Fig.4 was obtained by deriving kQ_{n-1} using Eq.5 then subtracting it from Eq.5. The other recursive forms were obtained in the same manner.

Fig. 4. Examples of routing equation applications.

Kernal Shape	Reccession Coefficient	λ_n	Routing Equation: Original Form	Routing Equation: Recursive Form	Remark
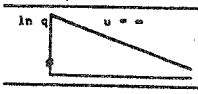	$k=k1_n=k2_n=k3_n$ for all n	$(1-k)$	$Q_n=\sum_{j=0}^{\infty} k^j\lambda I_{n-j}$	$Q_n=kQ_{n-1}+\lambda_n I_n$	single linear reservoir model
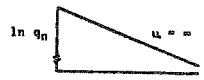	$k_n=k1_n=k2_n=k3_n$	$(1-k_n)$	$Q_n=\sum_{j=0}^{\infty} k_{n-j}^{j}\lambda_{n-j}I_{n-j}$	$Q_n=k_{n-1}Q_{n-1}+\lambda_n I_n + \sum_{j=2}^{\infty} k_{n-j}^{j-1}(k_{n-j}-k_{n-1})\lambda_{n-j}I_{n-j}$	single nonlinear reservoir model with single recession coefficient
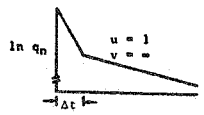	$k12_n$ $k2_n=k3_n$	$\frac{1-k2_n}{1-k2_n+k12_n}$	$Q_n=\lambda_n I_n+\sum_{j=1}^{\infty} k12_{n-j}k2_{n-j}^{j-1}\lambda_{n-j}I_{n-j}$	$Q_n=k12_{n-1}Q_{n-1}+\lambda_n I_n + \sum_{j=2}^{\infty} k12_{n-j}k2_{n-j}^{j-2}(k2_{n-j}-k12_{n-1})\lambda_{n-j}I_{n-j}$	single nonlinear reservoir model with double recession coefficients
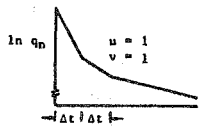	$k12_n$ $k23_n$ $k3_n$	$\frac{1-k3_n}{1-k3_n+k12_n-k12_nk3_n+k12_nk23_n}$	$Q_n=\lambda_n I_n+k12_{n-1}\lambda_{n-1}I_{n-1} + \sum_{j=2}^{\infty} k12_{n-j}k23_{n-j}k3_{n-j}^{j-2}\lambda_{n-j}I_{n-j}$	$Q_n=k23_{n-2}Q_{n-1}+\lambda_n I_n +(k12_{n-1}-k23_{n-2})\lambda_{n-1}I_{n-1} + \sum_{j=3}^{\infty} k12_{n-j}k23_{n-j}k3_{n-j}^{j-3}(k3_{n-j}-k23_{n-2})\lambda_{n-j}I_{n-j}$	single nonlinear reservoir model with triple recession coefficients

Because the third term in Eq.5 is infinite, for a practical computation, the portion of the total runoff described by the third term, i.e. the total third recession runoff, $Q3_n$, is separated into the two parts: the first element of the total third recession runoff, $Q3F_n$, and the sum of remaining elements, $Q3R_n$, as:

$$Q3F_n = k1_{n-(u+v)}^{u-1} \; k12_{n-(u+v)} \; k2_{n-(u+v)}^{v-1} \; k23_{n-(u+v)} \; \lambda_{n-(u+v)} \; I_{n-(u+v)} \tag{6}$$

$$Q3R_n = \sum_{j=u+v+1}^{\infty} k1_{n-j}^{u-1} \; k12_{n-j} \; k2_{n-j}^{v-1} \; k23_{n-j} \; k3_{n-j}^{j-u-v} \; \lambda_{n-j} \; I_{n-j} \tag{7}$$

By assuming $$Q3R_n = Q3_{n-1} \; k3^*_{n-1} \tag{8}$$

then $$Q3_n = Q3F_n + Q3_{n-1} \; k3^*_{n-1} \tag{9}$$

where $k3^*_{n-1}$ is the total third recession coefficient in period n-1 representing the ratio of the total third recession runoff in period n-1 to the total third recession runoff in period n if there is no new input into the total third recession runoff in period n, i.e. $Q3F_n=0$. If the function of the total third recession coefficient and the initial value of the total third recession runoff are known, the computation of the total third recession can be done recursively. The section on input data and parameters contains an example showing how recession periods and recession coefficients can be determined.

SOIL MOISTURE INPUT

The input, I_n, represents a depth of water available for runoff, and not the actual water input. Thus, a runoff coefficient is used to adjust the actual water input for losses such as evapotranspiration.

$$I_n = Rcf \; RLSE_n \tag{10}$$

where Rcf is a seasonal runoff coefficient, and RLSE is the water released into the basin, i.e., the water available at the soil surface, owing to rain and/or snowmelt. The value of the runoff coefficient can be determined using the ratio of seasonal runoff to seasonal precipitation. In the application of the model, one constant runoff coefficient is used throughout the entire snowmelt season. Although it is not included in Eq.10 for a simple explanation, the timing of the water release must be adjusted adequately according to the time lags.

The procedure used to determine the water releases is based on an inventory of the snowpack. The degree-day method is used to estimate snowmelt, and snowpack conditions (snow water equivalent and snowpack density) are simulated on a daily basis. Water released from the snow-covered and/or snow-free areas by rain and/or snowmelt over each elevation zone are obtained and then added for computing the total water released (RLSE).

An inventory of the snowpack is maintained over 20 equal-area elevation zones. From this inventoy, water releases from these elevation zones as well as snowcover over the basin can be estimated. For real time operation, the degree-day factor can be adjusted by comparing the computed with the observed snow-coverages on a seasonal basis.

Computation of melt volume or rainfall release from snowpack during the snowmelt period is complicated by the fact that the snowpack is not fully primed for some portion of the basin for some time periods. Thus for a certain period, the entire (or portion of) the basin is not capable of releasing water from the snowpack regardless of the temeprature. In this model, it has been assumed the snowpack in an elevation zone does not release water unless the snowpack is ripe. A ripe snowpack is defined to occur when the snowpack is ready to transmit and discharge liquid water entering at its surface, which is when it contains all the water which it can hold against gravity. These requirements are assumed to be the sum of the cold content, Wc, and the liquid-water-deficiency, Wd. First the cold content must be satisfied; then the liquid-water-deficiency.

Cold Content (Wc)

According to the Corps of Engineers (1956; p.144), night time snow crusts are confined to the top layers of the snowpack: generally 15 cm (6 inches) and seldom exceed 25 cm (10 inches) in thickness. In this model, it is assumed that a daily cold content is confined to the top 25 cm. To compute the daily cold content of the top 25 cm of the snowpack, An empirical relationship developed by the Corps of Engineers(1956; figure 1, plate 8-6), which relates the cold content of the top 60 cm of the snowpack to the average air temperature of the preceding 3 days, is adapted. To compute the cold content of the entire snowpack, the cold content of the previous day is updated by the cold content of the top 25 cm, Wc25, snowmelt and rain as:

$$Wc_n = Wc_{n-1} - MELT_n - RAIN_n + Wc25_n \qquad (11)$$
$$0 \le Wc_n \le WcMax_n$$

where MELT = snowmelt in cm of water,
RAIN = rainfall in cm,
Wc25 = cold content of the top 25 cm of the snowpack in cm of water,
Wcmax = potential maximum cold content in cm of water, and
n = day number.

Since the maximum cold content is likely to occur if the the entire snowpack condition is the same as the top 25 cm, the computed cold content is limited to this potential maximum cold content. The initial cold content is assumed as this potential maximum cold content with the average temperature of the previous month. It should be noted that modifications were made to the Corps of Engineers procedure to adapt it to this model without any experimental justification.

Liquid-water-deficiency

Eagleson (1970) stated: "Because of the many complex influences upon the snowpack water-holding-capacity, the liquid-water-deficiency cannot be expressed theoretically in terms of readily observable physical parameters. However, a large part of its variability can be accounted for by an empirical correlation with snowpack density."

For this model, the liquid-water-deficiency is assmued as a function of the density difference between the current snowpack and a hypothetical ripe snowpack. The hypothetical ripe snowpack is assumed to have a maximum snowpack density which can be fixed as a constant for the specified basin. The liquid-water-deficiency, Wd_n, is estimated by:

$$Wd_n = Wd_{n-1} - MELT_n - RAIN_n + Wdf_n \qquad (12)$$

$$Wdf_n = [(\rho max - \rho sf_n) / \rho w] \, SNOW_n \qquad (13)$$

where Wdf = liquid-water deficiency created by new snowfall in cm of water,
ρmax = maximum snowpack density in g/cm^3,
ρsf = density of the new snowfall in g/cm^3,
ρw = density of water, equal to 1.0 g/cm^3, and
n = day number.

Since a negative liquid-water-deficiency in Eq.12 represents a water release from the snowpack,

$$RLSE_n = \max(0., -Wd_n) \qquad (14)$$

where RLSE is the water released from the snowpack in cm of water. Indeed, the snowpack is ripe with varying snowpack densities, and the liquid-water-deficiency is changing depending on the metamorphosis of the snowpack. However, it should be noted that the assumptions used in Eq.12 and Eq.13 have not been verified.

Snowmelt by the Degree-day Method

A simple linear relationship (Martinec, 1960; Kuusisto, 1980), is used to account for the degree-day factor (Df).

$$MELT_n = Df_n \, T_n \tag{15}$$

$$Df_n = a \, \rho s_n \, / \, \rho w \tag{16}$$

where MELT = snowmelt in cm of water,

Df = degree-day factor in cm of water per ^{o}C-day,

T = degree(^{o}C)-days computed by the linear interpolation of daily maximum and minimum temperatures,

a = adjusting coefficient in cm of water per ^{o}C-day,

ρs = snowpack density in g/cc,

ρw = water density in g/cc, and

n = day number.

For this model, a is seasonally constant and determined by comparing computed snow-coverage with observed snow-coverage. A problem of using Eq.16 is estimation of the snowpack density over a large watershed. For this model, the snow density is estimated as a result of computing liquid-water-deficiency and snow water equivalent (SWE). Because SWE is a water balance of the snowpack, it can be computed as:

$$SWE_n = SWE_{n-1} - RLSE_n + PRCP_n \tag{17}$$

where PRCP indicates precipitation in cm of water. Using Eq.12 and Eq.13, the snowpack density can be updated by:

$$\rho s_n = \rho max - (\rho w \, Wd_n \, / \, SWE_n) \tag{18}$$

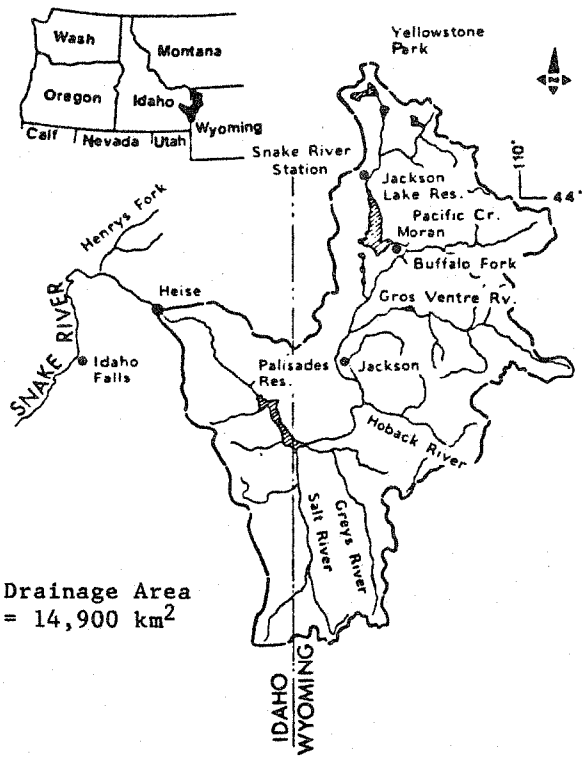

Fig. 5. The Upper Snake River basin above Heise.

STUDY AREA

The study basin lies between 109° 45' and 111° 45' west longitude and 42° 25' and 44° 30' north latitude within the States of Wyoming and Idaho as shown in Fig.5. This basin is 14,900 km² in area and rises from 1,524 m at the outlet to 4,197 m on the Grand Teton.

Average annual precipitation for the basin is about 920 mm for the eleven year period (1972-1982), and ranges from about 250 mm in the basin outlet to more than 1,250 mm in the high mountain ranges. On the high mountain ranges, high precipitation during the winter season forms extensive snow fields which furnish water for lower areas (Snake River Plain) during the summer dry season. Summers are moderately warm to hot and winters are severely cold.

Average annual runoff from the basin is 417 mm for the 72 year period (1911-1982), and usually the snowmelt runoff starts in late April and lasts until early July. During the test years (1972-1982), the average annual runoff was 440 mm, about 6 percent higher than the long-term average, and there were three very wet years (1972, 1974 and 1982) as well as three very dry years (1973, 1977 and 1981).

INPUT DATA AND PARAMETERS

Daily maximum and minimum temperatures and precipitation observed at Moran in Wyoming and the Snake River Station north of the Jackson Lake were averaged and used as indices for extrapolation. Estimated unregulated flows were obtained from the Corps of Engineers, Walla Walla District Office. Testing periods were limited to the eleven snowmelt seasons (April 1 to July 31, 1972 to 1982).

Temperature Lapse Rate

Seasonally varying lapse rates for minimum and maximum temperatures were developed for the basin. As shown in Fig.6, monthly lapse rates, which were estimated from the relationships between elevation and average monthly temperatures, were plotted and then smoothed by use of a Fourier-series.

Initial Snow Water Equivalent and Snow Density

Thirty-four snow courses located within the basin or near the basin, were selected to establish the relationship between the April 1 snow water equivalent (SWE) vs. elevation. To determine the relationship between SWE vs. elevation, the snow courses were weighted by considering the winter precipitation in the lower zones and the number of stations in each elevation zone (see Fig.7). The April 1 snow density at each snow course was computed from the snow depth and the SWE. The average densities of 1972 and 1978 were very high, 0.404 and 0.415 g/cm^3, while that of 1977 was very low, 0.246 g/cm^3. No paticular relationship was found between the snow desity and elevation so that the average density of all the snow courses was used each year. The maximum snowpack density, which was used in Eq.13 and Eq.18, was assumed as 0.42 g/cc, slightly higher than the maximum April 1 snowpack density in 1978, 0.415 g/cc.

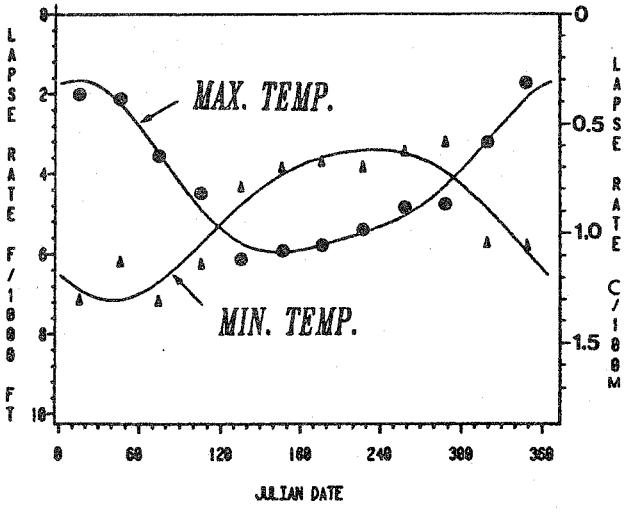

Fig. 6. Computed monthly lapse rates and seasonal curves of the maximum and minimum temperatures for the Upper Snake River basin above Heise.

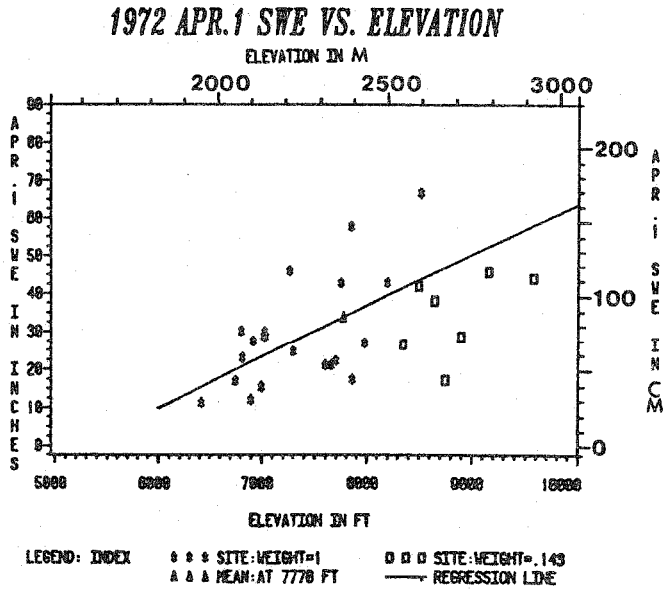

Fig. 7. April 1, 1972, snow water equivalents vs. elevation for the snow courses in the Upper Snake River basin.

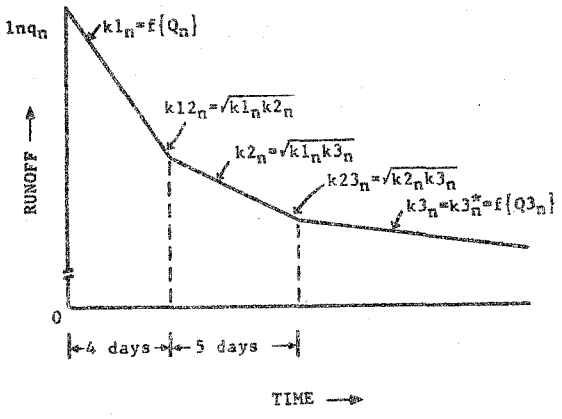

Fig. 8. Illustration of the daily runoff hydrograph for the Upper Snake River basin above Heise.

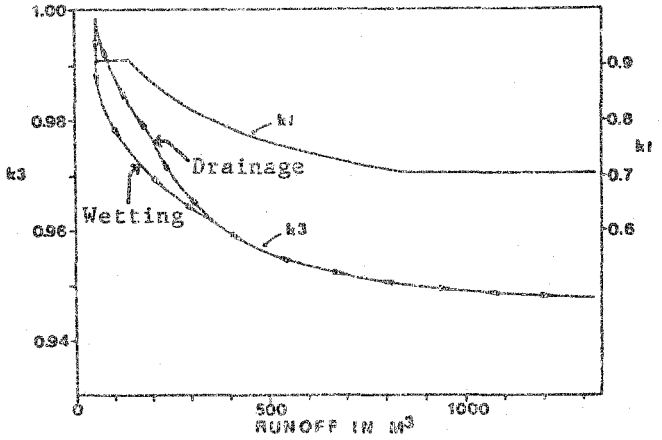

Fig. 9. Recession coefficient curves for the Upper Snake River basin above Heise. The first recession coefficient (k1) is a function of the total runoff and the third recess coefficient (k3) is function of the total third reccession runoff.

Recession Periods and Recession Coefficients

For each snowmelt season, there were one major and several minor peaks in runoff. Examination of the minor peaks indicated that recessions of these minor peaks lasted up to 9 days. For the first 4 days, these minor peaks decreased rapidly then decreased at a slightly slower rate for the following 5 days. Thus, the first recession period was assumed to be 4 days and the second recession period 5 days (Fig.8).

The total third recession coefficient, $k3^*$, represents a decreasing ratio of the total third recession runoff if no new runoff element enters into the third recession. Thus, characteristics of the third recession runoff can be found by examining the snowmelt recession runoff which occurs after the water input from snowmelt or rainfall has been ceased. Comparison of the last part of snowmelt hydrographs indicated that shapes of the recessions are almost the same, as a function of the runoff rates, for all the test seasons (1972-1982). For the 1974 season, there was an extremely high peak runoff, and little precipitation occurred during the recession period. These conditions resulted in a useful shape of the total third recession curve with minor distortions so that it was adopted for the basin.

During the snowmelt season, the basin absorbs some of the water input caused by snowmelt or rainfall. Thereafter it releases the water slowly from storage. This process may be analogous to hysteresis in the wetting and drainage process in a soil column. This characteristic of the hysteresis appears to exist in the snowmelt runoff especially for a semi-arid basin such as the study basin. Since the total third recession curve was derived for the drainage process, another recession curve was developed for the wetting period by using the winter minimum flow recession (see Fig.9).

For finding the first recession coefficient, it is necessary to separate the total hydrograph into "daily hydrographs" showing the distribution of the runoff only from one day's input. It would be the most difficult process because it would require determining the recession coefficients implicitly. Therefore, an empirical method was used to separate the total hydrograph into hydrographs representing only the minor peaks. The separation was made using the derived total third recession curve. Runoff in valleys between the minor peaks was assumed to decrease following the total third recession curve. The first recession function was then determined as a function of the total runoff by anlyzing these separate hydrographs and associated total runoff (Fig.9).

The third recession coefficient, $k3_n$, needs to be computed from the separated "daily hydrograph" because of the nonlinearity of in Eq.5. However, it was assumed to be the total third recession, i.e. $k3_n=k3^*_n$, by assuming that the nonlinearity is not significant for the third recession process. Other recession coefficients were assumed to be geometric means of the adjacent recession coefficients: $k2_n=(k1_n k3_n)^{1/2}$; $k12_n=(k1_n k2_n)^{1/2}$; $k23_n=(k2_n k3_n)^{1/2}$.

CALIBRATION, RESULTS AND DISCUSSIONS

The degree-day factor was adjusted using the coeffficient a in Eq.16 so that the computed snow cover closely matched that observed on a seasonal basis. The values for this coefficient are quite variable year-to-year (Tab.1). The runoff coefficient was also adjusted to match the computed seasonal runoff volume with the observed seasonal runoff volume. The average runoff coefficient was 0.41 with little year-to-year variation. It is significant to note that only these two factors were adjusted to calibrate the model for each season.

Table 1. Observed data and simulation results.

	Observed Data			Simulation Results			
Year	Seasonal Runoff (normal =100) %	Average Apr.1 SWE cm	Average Apr.1 Snow density g/cc	a cm/°C-day	Rcf -	R^2 -	Seasonal Volumetric Difference %
1972	137	85.9	0.40	1.6	0.41	0.98	<0.1
1973	87	49.5	0.30	1.7	0.39	0.94	0.7
1974	136	88.9	0.35	2.2	0.43	0.97	0.6
1975	115	69.9	0.31	1.7	0.41	0.91	-0.8
1976	124	89.4	0.35	1.8	0.40	0.93	0.9
1977	52	27.2	0.25	0.9	0.29	0.72	0.1
1978	120	82.6	0.42	1.4	0.41	0.96	0.5
1979	91	70.1	0.35	2.1	0.34	0.95	0.4
1980	97	65.5	0.32	1.8	0.40	0.89	-0.7
1981	79	35.1	0.28	1.4	0.47	0.83	-0.2
1982	137	90.9	0.36	2.5	0.42	0.86	-2.0

In Fig.10 through Fig.13, figures of observed and simulated snow-coverages, runoff, and separated runoff contributions are shown for extremely high (1974), high (1978), average (1980), and extremely low (1977) runoff years. The simulation of the snowcover indicated that there were significant errors during the early stages of the snowmelt seasons. These errors appeared to be due the absence of snow course data below 1,900 m coupled with frequent precipitation. Generally, the simulated snow-coverage was within 5 percent of observed values throughout each season. As shown in the observed and simulated runoff hydrographs, only minor differences exist in terms of timing and volume of runoff. However, some differences do exist especially when heavy precipitation occurred. It could be inferred that when heavy precipitation occurred during the middle of the snowmelt season, the snowpack accounting procedure used in this study was not fully capable of simulating the complicated snowpack metamorphosis. The three contributions to the total runoff as computed from the first, second, and third recession periods clearly illustrate the delay and attenuation phenomena of the routing structure in the model. The average contribution percentage for each recession period was 33, 15, and 52 percent from the first, second and third recession periods, respectively, and as expected, the greatest deviations from these values occurred in the extremely dry 1977 season. It should be noted that these figures simply show the runoff contributions from the different recession periods and not from different paths. Thus, they should not be compared directly with "path-oriented" terms (e.g. surface, subsurface and baseflow).

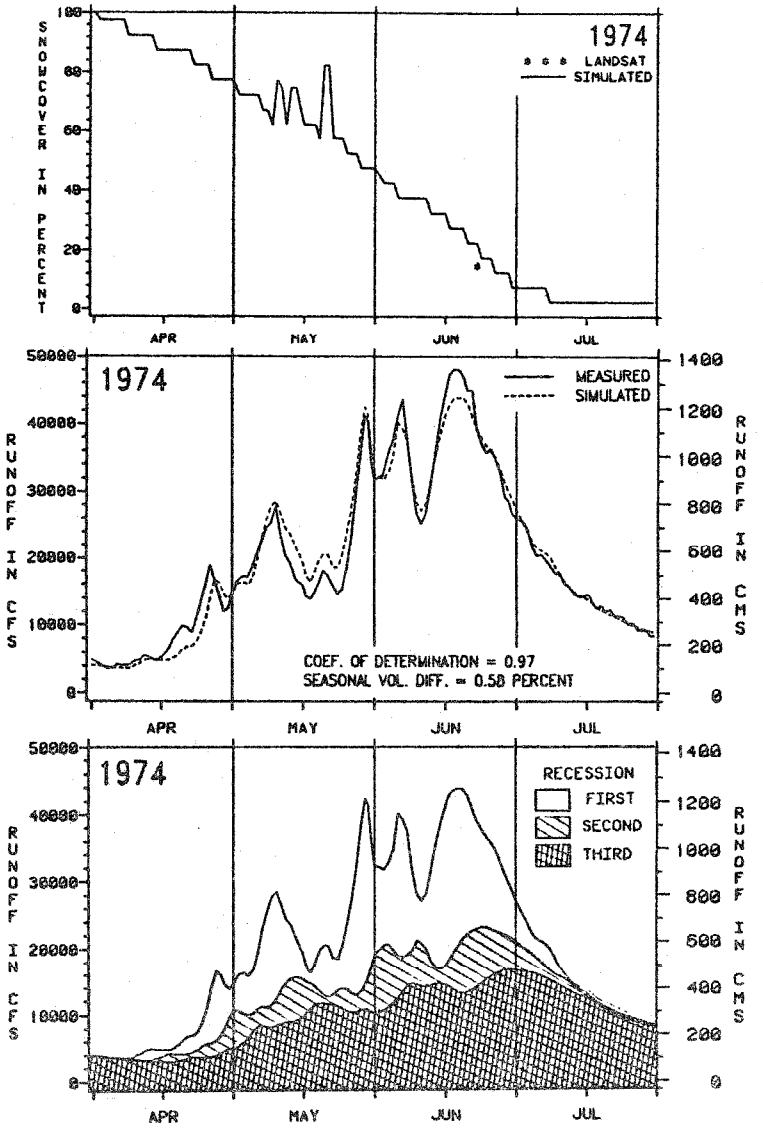

Fig. 10. Simulated and observed snow-coverages and runoff, and simulated separated runoff contributions for the 1974 snowmelt season.

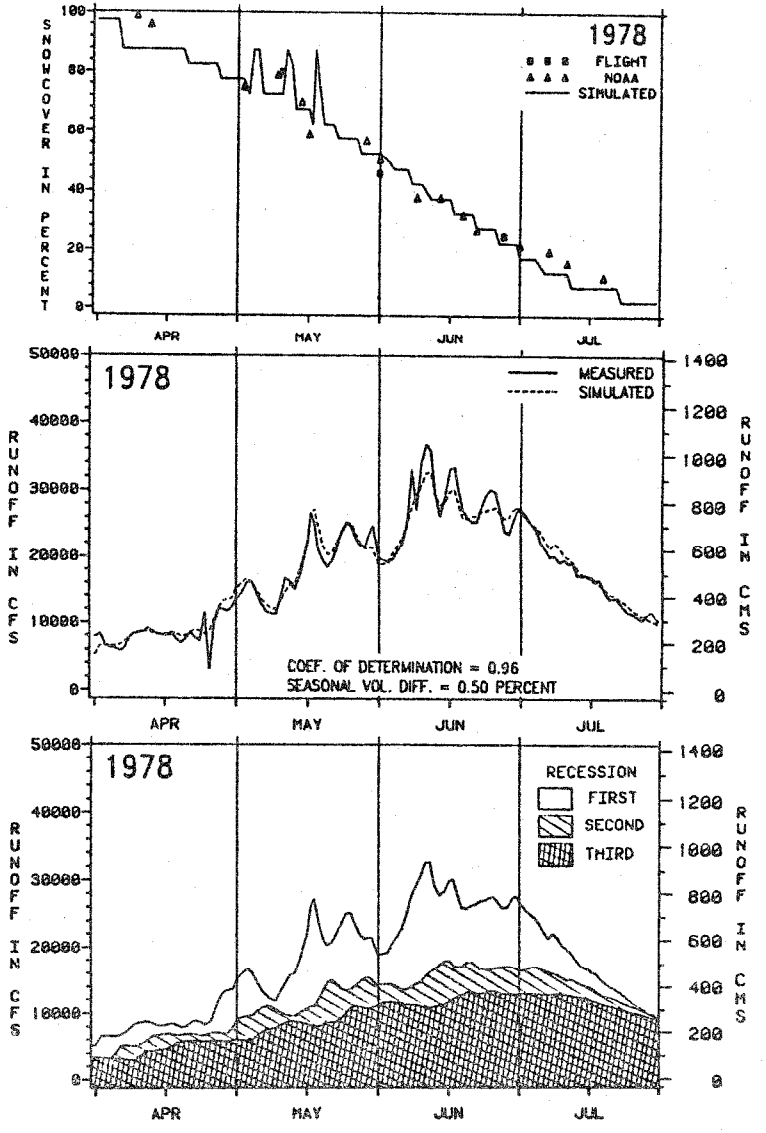

Fig. 11. Simulated and observed snow-coverages and runoff, and simulated separated runoff contributions for the 1978 snowmelt season.

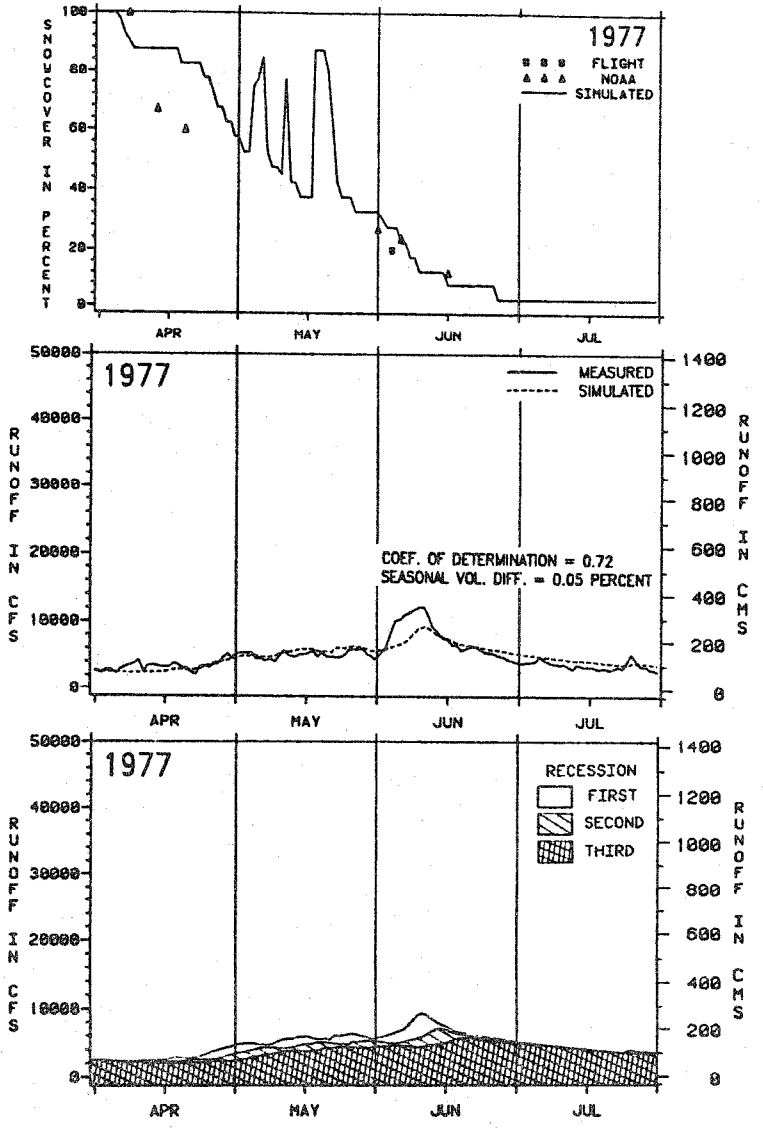

Fig. 12. Simulated and observed snow-coverages and runoff, and simulated separated runoff contributions for the 1977 snowmelt season.

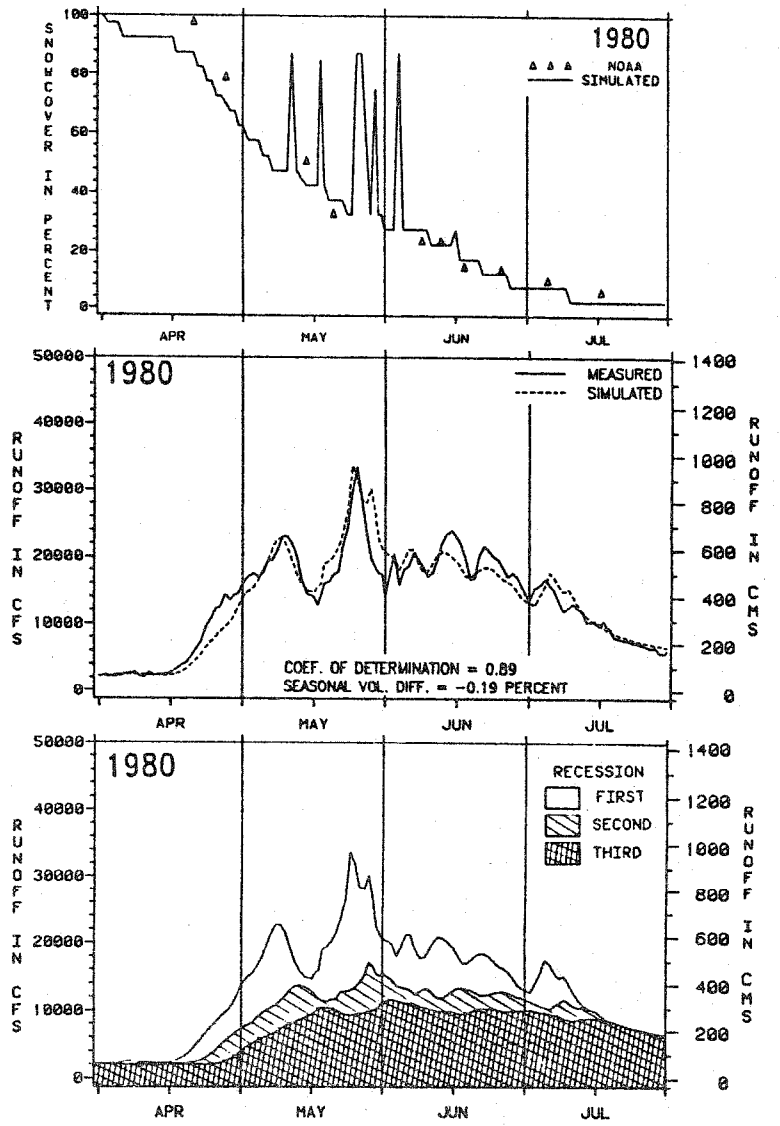

Fig. 13. Simulated and observed snow-coverages and runoff, and simulated separated runoff contributions for the 1980 snowmelt season.

Generally the simulation results appear to be acceptable for operational purposes as shown in Tab.1. For the eleven snowmelt seasons, the average volumetric differences between the computed and the observed were less than one percent and the average coefficient of determination (R^2) was 0.91.

SUMMARY AND CONCLUSIONS

1. A generalized hydrograph equation was derived by using the well known concepts of superimposition and nonlinear multiple recessions; Characteristics of delay and attenuation of the runoff process were effectively accounted for through the use of the equation.
2. Oserved snowcover was closely simulated by the snowmelt procedure, and the observed snowcover data were used to adjust the degree-day factor.
3. A simplification of the common conceptual watershed modeling appeared to be possible by using the derived equation while maintaining the characteristics of the runoff process.
4. Further testing is necessary to verify the procedures under a variety of conditions.

ACKNOWLEDGEMENTS

Financial support for the work reported in this paper was provided by the Idaho Department of Water Resources Water District 01, U.S. Bureau of Reclamation, and the Corps of Engineers. The authors are grateful to Peter L. Palmer and Jerald A. Beard, Soil Conservation Service, Boise for providing snow survey data.

REFERENCES

Barnes, B. S. 1939. The structure of discharge - Recession curves. Trans. American Geophysical Union, Part IV. P. 721-725.

Corps of Engineers. 1956. Snow Hydrology. North Pacific Division, Portland, Oregon.

Dunne, T. and R. Black. 1971. Runoff process during snowmelt. Water Resources Research 7(5):1160-1172.

Eagleson, P. S. 1970. Dynamic hydrology. McGraw-Hill Book Company, New York. p. 250.

Garstka, W. U., L. D. Love, B. C. Goodell, and F. A. Bertle. 1958. Factors affecting snowmelt and streamflow. U.S. Bureau of Reclamation and Forest Service, Washington, D.C. 189 p.

Kim, S. 1986. Daily irrigation supply and demand simulation for a basin-wide irrigation. Unpublished Ph.D. dissertation, University of Idaho, Moscow. (In progress).

Klemeš, V. 1983. Conceptualization and scale in hydrology. Journal of Hydrology 65(1/3):1-23.

Kuusisto, E. 1980. On the values and variability of degree-day melting factor in Finland. Nordic Hydrology 11(5):235-242.

Martinec, J. 1960. The degree-day factor for snowmelt-runoff forecasting. Proceedings of the International Association of Scientific Hydrology, General Assembly of Helsinki, Commission of Surface Waters. p. 468-477.

Martinec, J. 1963. Forecasting streamflow from snow storage in an experimental watershed. Proceedings of the International Association of Scientific Hydrology, General Assembly of Berkeley, Symposium of Surface Waters. p. 127-134.

Martinec, J. 1965. A representative watershed for the research of snowmelt-runoff relations. Proceedings of the International Association of Scientific Hydrology, General Assembly of Budapest. p. 494-501.

Martinec, J. 1975. Snowmelt-runoff model for stream flow forecasts. Nordic Hydrology 6(3):145-154.

Martinec, J., A. Rango., and E. Major. 1983. The Snowmelt-Runoff Model (SRM) user's manual. NASA Reference Publication No. 1100. 118 p.

Rango, A. and J. Martinec. 1981. Accuracy of snowmelt runoff simulation. Nordic Hydrology 12(4/5):265-274.

Raudkivi, A. J. 1979. Hydrology. Pergamon Press Inc., New York.

Toebes, C. and D. D. Strang. 1964. On recession curves - 1. Recession equations. J. of Hydrology, N.Z. 3(2):2-15.